

See discussions, stats, and author profiles for this publication at: <https://www.researchgate.net/publication/244449878>

3-Aryl[1,2,4]triazino[4,3-*a*]benzimidazol-4(10*H*)-ones: A New Class of Selective A₁ Adenosine Receptor Antagonists

ARTICLE in JOURNAL OF MEDICINAL CHEMISTRY · FEBRUARY 2001

Impact Factor: 5.45 · DOI: 10.1021/jm001054m

CITATIONS

53

READS

7

10 AUTHORS, INCLUDING:



Sabrina Taliani

Università di Pisa

85 PUBLICATIONS 1,065 CITATIONS

SEE PROFILE



Concettina La Motta

Università di Pisa

105 PUBLICATIONS 1,354 CITATIONS

SEE PROFILE



Ettore Novellino

University of Naples Federico II

618 PUBLICATIONS 9,099 CITATIONS

SEE PROFILE



Antonio Lavecchia

University of Naples Federico II

119 PUBLICATIONS 2,480 CITATIONS

SEE PROFILE

3-Aryl[1,2,4]triazino[4,3-*a*]benzimidazol-4(10*H*)-ones: A New Class of Selective A₁ Adenosine Receptor Antagonists

Federico Da Settimo,^{*,§} Giampaolo Primofiore,[§] Sabrina Taliani,[§] Anna Maria Marini,[§] Concettina La Motta,[§] Ettore Novellino,[‡] Giovanni Greco,[‡] Antonio Lavecchia,[‡] Letizia Trincavelli,[⊥] and Claudia Martini[⊥]

Dipartimento di Scienze Farmaceutiche, Università di Pisa, Via Bonanno 6, 56126 Pisa, Italy, Dipartimento di Chimica Farmaceutica e Tossicologica, Università di Napoli "Federico II", Via D. Montesano, 49, 80131 Napoli, Italy, and Dipartimento di Psichiatria, Neurobiologia, Farmacologia e Biotecnologie, Università di Pisa, Via Bonanno 6, 56126 Pisa, Italy

Received August 7, 2000

Radioligand binding assays using bovine cortical membrane preparations and biochemical in vitro studies revealed that various 3-aryl[1,2,4]triazino[4,3-*a*]benzimidazol-4(10*H*)-one (ATBI) derivatives, previously reported by us as ligands of the central benzodiazepine receptor (BzR) (Primofiore, G.; et al. *J. Med. Chem.* **2000**, *43*, 96–102), behaved as antagonists at the A₁ adenosine receptor (A₁AR). Alkylation of the nitrogen at position 10 of the triazinobenzimidazole nucleus conferred selectivity for the A₁AR vs the BzR. The most potent ligand of the ATBI series (10-methyl-3-phenyl[1,2,4]triazino[4,3-*a*]benzimidazol-4(10*H*)-one **12**) displayed a *K_i* value of 63 nM at the A₁AR without binding appreciably to the adenosine A_{2A} and A₃ nor to the benzodiazepine receptor. Pharmacophore-based modeling studies in which **12** was compared against a set of well-established A₁AR antagonists suggested that three hydrogen bonding sites (HB1 acceptor, HB2 and HB3 donors) and three lipophilic pockets (L1, L2, and L3) might be available to antagonists within the A₁AR binding cleft. According to the proposed pharmacophore scheme, the lead compound **12** engages interactions with the HB2 site (via the N2 nitrogen) as well as with the L2 and L3 sites (through the pendant and the fused benzene rings). The results of these studies prompted the replacement of the methyl with more lipophilic groups at the 10-position (to fill the putative L1 lipophilic pocket) as a strategy to improve A₁AR affinity. Among the new compounds synthesized and tested, the 3,10-diphenyl[1,2,4]triazino[4,3-*a*]benzimidazol-4(10*H*)-one (**23**) was characterized by a *K_i* value of 18 nM which represents a 3.5-fold gain of A₁AR affinity compared with the lead **12**. A rhodopsin-based model of the bovine adenosine A₁AR was built to highlight the binding mode of **23** and two well-known A₁AR antagonists (**III** and **VII**) and to guide future lead optimization projects. In our docking simulations, **23** receives a hydrogen bond (via the N1 nitrogen) from the side chain of Asn247 (corresponding to the HB1 and HB2 sites) and fills the L1, L2, and L3 lipophilic pockets with the 10-phenyl, 3-phenyl, and fused benzene rings, respectively.

Introduction

We have recently described the synthesis and the biological evaluation of 3-aryl[1,2,4]triazino[4,3-*a*]benzimidazol-4(10*H*)-ones (ATBIs, **1–17** in Table 1) as ligands of the benzodiazepine receptor (BzR).¹ While these compounds were under investigation, it was realized that they were structurally related to well-known potent A₁ adenosine receptor (A₁AR) antagonists (**I–VIII**)^{2–10} such as those shown in Figure 1. ARs have been identified by pharmacological and molecular biological techniques and classified into A₁, A_{2A}, A_{2B}, and A₃ subtypes, all belonging to the G-protein coupled receptors superfamily.^{11–13} Since selective A₁AR antagonists have demonstrated promising therapeutic potential for the treatment of cognitive diseases, renal failure, Alzheimer's disease, and cardiac failure,¹⁴ we

addressed the question of whether our ATBI derivatives could be targeted at the A₁AR. Several theoretical studies have improved our understanding of how AR ligands interact selectively with their binding sites,^{15–23} thus providing a solid background to predict the likelihood for a given structure to behave as agonist or antagonist at any of the ARs. A molecular modeling analysis confirmed that ATBIs are superimposable on A₁AR antagonists **I–VIII** about pharmacophoric elements required for high A₁AR potency (Figure 2).

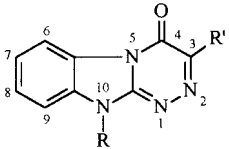
Given the role of the N10-H group as a hydrogen bond donor at the BzR¹ but not at the A₁AR (as established by the modeling studies), we predicted that N10-alkyl derivatives might be A₁AR selective ligands devoid of appreciable affinity at the BzR. Expectedly, several of our compounds were found to act as A₁AR antagonists without binding to the BzR. The above-mentioned pharmacophore-based overlay was successfully exploited to design novel ATBI derivatives with improved potency at the A₁AR. Finally, we built a model of the bovine A₁AR to rationalize the SARs of ATBI ligands and to facilitate, perspectively, the design of new analogues.

* To whom all correspondence should be addressed. Tel: 39 50 500209. Fax: 39 50 40517. E-mail: fsettimo@farm.unipi.it.

§ Dipartimento di Scienze Farmaceutiche, Università di Pisa.

‡ Dipartimento di Chimica Farmaceutica e Tossicologica, Università "Federico II" di Napoli.

⊥ Dipartimento di Psichiatria, Neurobiologia, Farmacologia e Biotecnologie, Università di Pisa.

Table 1. Affinity of ATBI Derivatives at Bovine Brain A₁, A_{2A}, and A₃ARs


no.	R	R'	K _i (nM) or % inhibition ^a		
			bA ₁ ^b	bA _{2A} ^c	bA ₃ ^d
1	H	H	34%	0%	
2	H	CH ₃	3900 ± 280	39%	
3	H	C ₆ H ₅	85 ± 7.2	2900 ± 190	5%
4	H	C ₆ H ₄ -4'-Cl	44%	8%	
5	H	C ₆ H ₄ -4'-OCH ₃	30%	16%	
6	H	C ₆ H ₄ -4'-OH	249 ± 23	1300 ± 121	
7	H	C ₆ H ₃ -3',4'-(OCH ₃) ₂	1780 ± 150	35%	
8	H	C ₆ H ₃ -3',4'-(OH) ₂	470 ± 43	3500 ± 290	
9	H	fur-2-yl	261 ± 24	241 ± 23	
10	H	thien-2-yl	293 ± 26	1023 ± 95	
11	H	thien-3-yl	119 ± 10	5000 ± 470	
18	CH ₃	H	0%	8%	
19	CH ₃	CH ₃	46%	0%	
12	CH ₃	C ₆ H ₅	63 ± 5.4	25%	0%
13	CH ₃	C ₆ H ₄ -4'-Cl	66%	0%	
14	CH ₃	C ₆ H ₄ -4'-OCH ₃	2050 ± 190	7%	
20	CH ₃	C ₆ H ₄ -4'-OH	206 ± 18	43%	
15	CH ₃	C ₆ H ₃ -3',4'-(OCH ₃) ₂	24%	18%	
21	CH ₃	C ₆ H ₃ -3',4'-(OH) ₂	459 ± 41	32%	
16	CH ₃	fur-2-yl	813 ± 70	6300 ± 610	
17	CH ₃	thien-2-yl	233 ± 21	19%	
22	CH ₃	thien-3-yl	78 ± 6.2	55%	
23	C ₆ H ₅	C ₆ H ₅	18 ± 2	18%	2%
24	C ₆ H ₅	fur-2-yl	315 ± 31	56%	
25	CH ₂ -C ₆ H ₅	C ₆ H ₅	274 ± 25	62%	13%
26	CH ₂ -C ₆ H ₅	C ₆ H ₄ -4'-OH	344 ± 33	1200 ± 110	
27	CH ₂ -C ₆ H ₅	fur-2-yl	990 ± 87	1236 ± 112	
28	CH ₂ -C ₆ H ₅	thien-3-yl	446 ± 41	60%	
DPCPX			0.5 ± 0.03	337 ± 28	>10000
NECA			14 ± 4	16 ± 3	73 ± 5
Cl-IBMECA			890 ± 61	401 ± 25	0.22 ± 0.02

^a The K_i values are means ± SEM of four separate assays, each performed in triplicate. ^b Displacement of specific [³H]CHA binding in bovine cortical membranes or percentage of inhibition (%) of specific binding at 10 μM concentration. ^c Displacement of specific [³H]CGS 21680 in bovine striatal membranes or percentage of inhibition (%) of specific binding at 10 μM concentration. ^d Displacement of specific [¹²⁵I]AB-MECA binding to bovine cortical membranes in the presence of 20 nM DPCPX or percentage of inhibition (%) of specific binding at 1 μM concentration. Only compounds **3**, **12**, **23**, and **25** were tested.

Results and Discussion

Comparison of ATBI Derivatives with Known A₁AR Antagonists. Molecular modeling studies were performed to verify whether compound **12**, selected as a representative of the ATBI series, possessed pharmacophoric elements of well-known A₁AR antagonists (compounds **I–VIII** in Figure 1). Computational details are given in the Experimental Section. The points used for superimposing structures **I–VIII** and **12** are denoted in Figure 1 by bold labels (atoms supposed to make hydrogen bonds with the receptor) and dots (centroids of aromatic rings assumed to fit into hydrophobic regions of the binding site). Compounds **I–VII** were first aligned about the three atoms in bold (N or O, N, and H), keeping the orientation of the structural formulas adopted in Figure 1. Compound **VIII**, lacking the third hydrogen bonding atom, was overlayed on **VII** by matching the corresponding N and H atoms plus the pendant phenyl. Compound **12** was superimposed on

VII through the fitting of the nitrogen closest to the pendant phenyl plus the two benzene rings.

The alignment of compounds **I–VIII** and **12** (see Figure 2) suggests that, in addition to three putative hydrogen bonding sites (HB1 acceptor, HB2, and HB3 donors), three lipophilic pockets (L1, L2, and L3) might be available to antagonists within the A₁AR binding cleft.

Our pharmacophore model is similar to that proposed by Dooley and co-workers,²⁴ except for the HB3 site which has no equivalent in the latter model and for the alignment of some ligands.²⁵ As an example, **VIII** was oriented by Dooley et al. with the NH₂ group engaging the HB2 site and with the pendant, fused, and benzylic benzene rings fitting into the L1, L2, and L3 regions, respectively.

Differently from what was hypothesized to occur at the BzR,¹ the N10-H group of ATBIs does not make any hydrogen bonds at the A₁AR. Consequently, derivatives lacking the N10-H function should retain affinity to the A₁AR and lack potency at the BzR. These results strongly supported the screening of ATBI derivatives as A₁AR antagonists and provided the rationale to design new compounds with improved potency and selectivity in binding to the A₁AR vs the BzR.

Biological Evaluation of Compounds 1–22. To better delineate the SARs of ATBI derivatives, five new compounds (**18–22**), with respect to those described as BzR ligands (**1–17**),¹ were prepared by reacting 1-methyl-2-hydrazinobenzimidazole **29**²⁶ with the appropriate glyoxylic acids following experimental procedures similar to those previously reported to obtain the corresponding N10-H analogues **1**, **2**, **6**, **8**, and **11**¹ (Scheme 1, Tables 2 and 3). All the compounds **1–22** (Table 1) were tested in radioligand binding assays to determine their affinities at the bovine A₁, A_{2A}, and A₃ARs. In particular, affinities for A₁ and A_{2A}ARs were determined in competition assays of [³H]-N⁶-cyclohexyladenosine ([³H]CHA) and [³H]-2-[[4-(2-carboxyethyl)phenethyl]-amino]-5'-(N-ethylcarbamoyl)adenosine ([³H]CGS 21680) to bovine cortical (A₁) and striatal (A_{2A}) membranes, respectively. Moreover, to determine the intrinsic activity of the most A₁AR active compounds **3**, **12**, **23**, and **25**, competition studies were performed in the presence and in the absence of 1 mM GTP using the radiolabeled antagonist [³H]1,3-dipropyl-8-cyclopentylxanthine ([³H]-DPCPX).²⁷ The GTP shift is an in vitro parameter often indicative of intrinsic activity. In Table 4 the GTP shift values of the selected ATBIs and R-PIA, included as agonist reference compound, were reported. Affinity for A₃ARs was determined in competition assays of [¹²⁵I]-N⁶-(3-iodo-4-aminobenzyl)-5'-N-methylcarboxamido-adenosine ([¹²⁵I]AB-MECA) to bovine cortical membranes in the presence of the A₁AR selective antagonists DPCPX (20 nM). As reported for mouse cortical membranes,²⁸ to ascertain the validity of the used method in bovine cortical membranes, DPCPX competition studies of 1 nM [¹²⁵I]AB-MECA binding and [¹²⁵I]AB-MECA saturation isotherm in the absence and presence of DPCPX were carried out. [¹²⁵I]AB-MECA specific binding consisted of two components, since the A₁ selective antagonist DPCPX completely deleted the most but not all of the binding with high affinity (sigmoidal, monophasic curve had a K_i value of 0.22 nM). Then, the

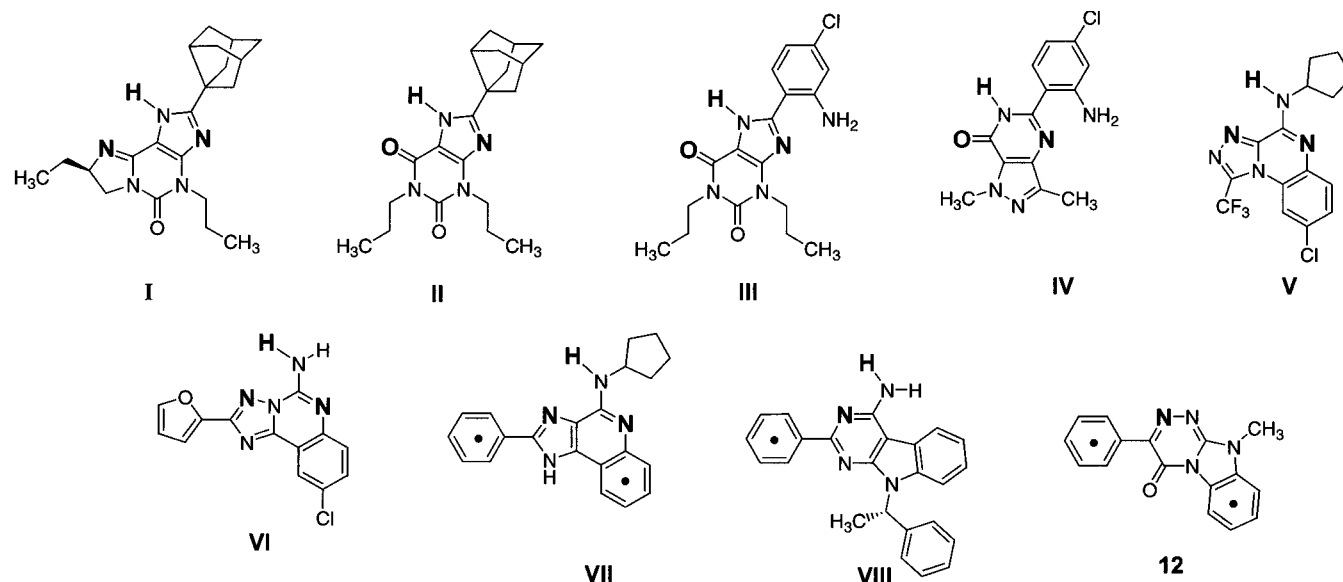


Figure 1. Compounds **I–VIII** are A₁AR antagonists reported in the literature that were used, together with the ATBI derivative **12**, to generate the pharmacophore model shown in Figure 2. Atoms in bold and dots served as fitting points. **I–VIII** are described in the following references: **I**,² **II**,^{3,4} **III**,⁵ **IV**,⁶ **V**,⁷ **VI**,⁸ **VII**,⁹ and **VIII**.¹⁰

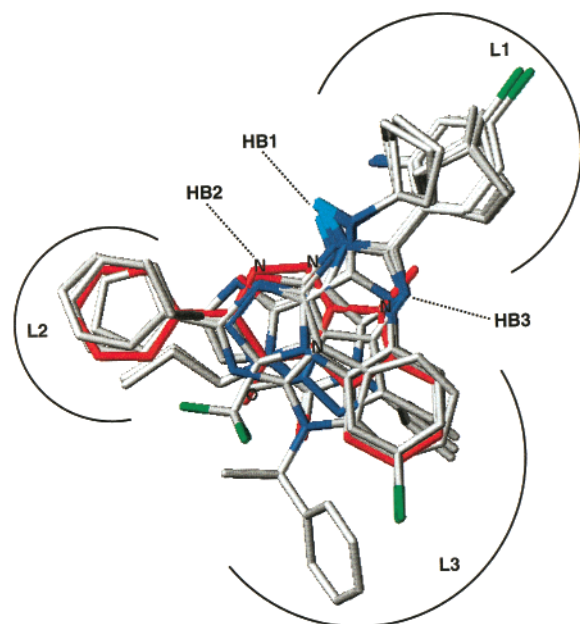
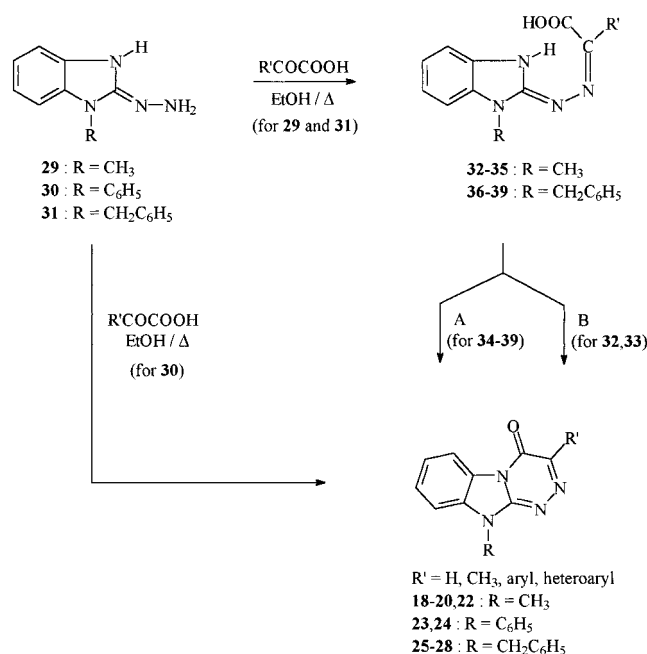


Figure 2. Molecular models of **I–VIII** and **12** (red) overlaid about the pharmacophoric points indicated in Figure 1 through bold labels and dots. Three putative hydrogen bonding sites (HB1 acceptor, HB2 and HB3 donors) and three lipophilic pockets (L1, L2, and L3) are hypothesized to exist within the A₁AR binding cleft.

residual binding which was not displaced by DPCPX at concentrations as high as 20 nM (about 100-fold above the K_i value to A₁AR) represented binding to A₃AR. Scatchard analysis of [¹²⁵I]AB-MECA binding, performed in the presence of 20 nM DPCPX, showed an affinity constant value of 1.02 ± 0.08 nM, and a maximum density of binding sites of 14.7 ± 1.2 fmol/mg of proteins according to the data reported for A₃AR in mouse brain.²⁸ In Table 1, the affinity constants values obtained in our experimental conditions for the selected agonists 5'-N-ethylcarboxamidoadenosine (NECA) and 2-chloro-N⁶-(3-iodobenzyl)adenosine (Cl-IBMECA), and the antagonist DPCPX as standards, were reported.

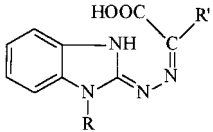
Scheme 1^a



^a Reagents: (A) ethanol, gaseous HCl, reflux; (B) glacial acetic acid, reflux.

In agreement with the results of the molecular modeling studies, several compounds (**3**, **6**, **8–11** and **12**, **16**, **17**, **20–22**) exhibited submicromolar affinity at the A₁AR. All the compounds, except **9**, showed a different degree of selectivity for the A₁AR compared with the A_{2A} and A₃ARs.

A crucial requirement for binding to the A₁AR is an aromatic ring at the 3-position, since 3-unsubstituted or 3-methylated ATBIs are devoid of affinity or scarcely active (**1**, **2**, **18**, and **19**). As predicted by our pharmacophore model, the presence or absence of a methyl group at the imidazole nitrogen N10 does not significantly influence affinity to the A₁AR as N10-H and N10-CH₃ derivatives are practically equipotent, with the exception of **9** and **16**. The most active compounds are

Table 2. Physical Properties and Spectral Data of Benzimidazol-2-ylhydrazone Derivatives **32–35** and **36–39**


no.	R	R'	yield (%)	mp (°C)	formula ^a	IR (cm ⁻¹)	¹ H NMR (ppm)	MS <i>m/e</i> (%)
32	CH ₃	H	65	175–177	C ₁₀ H ₁₀ N ₄ O ₂	3200–2800, 1670, 1570, 1240, 1070, 740	3.50 (s, 3H, CH ₃); 7.01–7.29 (m, 4H, Ar-H), 7.34 (s, 1H, 2-H)	218 (11, M ⁺); 200 (2); 174 (85); 131 (88); 44 (100)
33	CH ₃	CH ₃	86	200–202	C ₁₁ H ₁₂ N ₄ O ₂ ^b	3300–2600, 1710, 1640, 1320, 1110, 740	2.07 (s, 3H, 2-CH ₃); 3.51 (s, 3H, N-CH ₃); 6.99–7.30 (m, 4H, Ar-H)	232 (1, M ⁺); 214 (1); 187 (2); 131 (3); 45 (100)
34	CH ₃	C ₆ H ₄ -4'-OH	71	212–215 (dec)	C ₁₆ H ₁₄ N ₄ O ₃	3600–2400, 1650, 1600, 1270, 840, 740	3.52 (s, 3H, CH ₃); 6.77 (d, 2H, 3',5'-H); 7.05–7.35 (m, 4H, Ar-H); 7.71 (d, 2H; 2',6'-H)	310 (1, M ⁺); 292 (28); 264 (10); 147 (40); 119 (100)
35	CH ₃	thien-3-yl	66	228–231	C ₁₄ H ₁₂ N ₄ O ₂ S	3050–2300, 1600, 1580, 1450, 1080, 750	3.59 (s, 3H, CH ₃); 7.11–8.23 (m, 7H, Ar-H); 12.10 (bs, 1H, COOH)	300 (6, M ⁺); 282 (12); 256 (28); 147 (100)
36	CH ₂ C ₆ H ₅	C ₆ H ₅	72	189–192 (dec)	C ₂₂ H ₁₈ N ₄ O ₂	3200–2400, 1620, 1590, 1440, 740	5.24 (s, 2H, CH ₂); 7.03–7.87 (m, 14H, ArH)	352 (15, M ⁺ -H ₂ O); 324 (1); 222 (1); 91 (100)
37	CH ₂ C ₆ H ₅	C ₆ H ₄ -4'-OH	50	203–205	C ₂₂ H ₁₈ N ₄ O ₃	3400–2400, 1660, 1270, 730	5.19 (s, 2H, CH ₂); 6.75 (d, 2H, 3',5'-H); 7.00–7.52 (m, 9H, Ar-H); 7.68 (d, 2H, 2',6'-H); 9.54 (s, 1H, OH, exch. with D ₂ O)	368 (32, M ⁺ -H ₂ O); 342 (16); 222 (20); 91 (100)
38	CH ₂ C ₆ H ₅	fur-2-yl	71	201–202	C ₂₀ H ₁₆ N ₄ O ₃	1640, 1600, 1260, 1110, 740	5.31 (s, 2H, CH ₂); 6.53–6.60 (m, 1H, 4'-H); 7.09–7.45 (m, 10H, Ar-H); 7.72 (d, 1H, 5'-H); 12.20 (bs, 1H, COOH, exch. with D ₂ O)	360 (1, M ⁺); 222 (7); 91 (100)
39	CH ₂ C ₆ H ₅	thien-3-yl	76	143–145	C ₂₀ H ₁₆ N ₄ O ₂ S	3500–2600, 1640, 1600, 1260, 1120, 730	5.30 (s, 2H, CH ₂); 7.11–7.54 (m, 10H, Ar-H); 7.88 (dd, 1H, Ar-H); 8.15 (dd, 1H, Ar-H); 12.20 (bs, 1H, COOH, exch. with D ₂ O)	376 (1, M ⁺); 358 (48); 33 (8); 222 (11); 91 (100)

^a Elemental analyses for C, H, N, were within $\pm 0.4\%$ of the calculated values. ^b Literature ref 82.

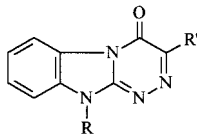
those bearing an unsubstituted phenyl ring at the 3-position (**3** and **12** with K_i values of 85 and 63 nM, respectively). Any substituent on the side phenyl ring decreases or abolishes affinity, thus suggesting that the lipophilic site of the A₁AR hosting the phenyl moiety (the L2 region in Figure 2) is relatively small. The only substituents tolerated on this ring were *meta* and *para* hydroxyls (compare **6**, **8**, **20**, and **21** vs **3** and **12**). The replacement of the side phenyl ring with a less bulky heteroaromatic five-membered ring, such as furyl or thienyl, gave compounds **9–11**, **16**, **17**, and **22**, showing an affinity only slightly lower than that of **3** and **12**.

Lead Optimization: Design, Synthesis, and Testing of New ATBI Derivatives. Inspection of the molecular alignment shown in Figure 2 suggested that affinity of the lead compound **12** ($K_i = 63$ nM) could be improved by replacing the methyl group at the N10-position with larger and hydrophobic substituents capable of filling the L1 lipophilic pocket. Accordingly, we synthesized and tested a number of N10-phenyl (**23**, **24**) and N10-benzyl (**25–28**) derivatives.

The new compounds **23**, **24**, and **25–28** were prepared starting from the appropriate 2-hydrazinobenzimidazole derivatives **30** and **31**, respectively (Scheme 1). 1-Ben-

zyl-2-hydrazinobenzimidazole **31** was obtained by a synthetic procedure reported in the literature.²⁶ We used the same procedure to prepare the already described 2-hydrazino-1-phenylbenzimidazole **30**²⁹ from hydrazine hydrate and 2-chloro-1-phenylbenzimidazole. This last compound was obtained by reaction of 1-phenylbenzimidazol-2-one and phenylphosphonic dichloride³⁰ at 170 °C with a better yield (60%) than that reported by Iemura (50%) by using POCl₃.³¹ 1-Phenylbenzimidazol-2-one was prepared in quantitative yield using a convenient modification of the procedure of Clark and Pessolano,³² i.e., employing triphosgene (bis-trichloromethyl carbonate)³³ instead of phosgene for the reaction of carbonylation of *N*-phenyl-1,2-phenyldiamine.

The reaction of 1-benzyl-2-hydrazinobenzimidazole **31** with the appropriate glyoxylic acids in ethanol, at reflux, furnished the intermediate 2-(benzimidazol-2-ylhydrazono)-2-substituted acetic acids **36–39** (Scheme 1, Table 2), which were purified by suspension in hot methanol as the recrystallization process always led to partial cyclization of the products. The cyclization of these acids was obtained using one of the following two methods (Scheme 1, Table 3): (A) by saturating with anhydrous hydrogen chloride a suspension of the acid in absolute

Table 3. Physical Properties and Spectral Data of Triazinobenzimidazole Derivatives **18–22**, **23**, **24**, and **25–28**


no.	R	R'	react. procd	yield (%)	recryst solv	mp (°C)	formula ^a	IR (cm ⁻¹)	¹ H NMR (ppm)	MS <i>m/e</i> (%)
18	CH ₃	H	B	32	MeOH	206–207	C ₁₀ H ₈ N ₄ O	1700, 1680, 1250, 980, 750, 730	3.84 (s, 3H, CH ₃); 7.37–7.76 (m, 3H, Ar-H); 8.26 (s, 1H, 3-H); 8.34 (dd, 1H, 6-H)	200 (100, M ⁺); 144 (41); 118 (39)
19	CH ₃	CH ₃	B	31	MeOH	225–226	C ₁₁ H ₁₀ N ₄ O ^b	1670, 1570, 1460, 1090, 760, 740	2.41 (s, 3H, 3-CH ₃); 3.76 (s, 3H, N-CH ₃); 7.29–7.67 (m, 3H, Ar-H); 8.29 (dd, 1H, 6-H)	214 (100, M ⁺); 186 (22); 144 (65); 118 (67)
20	CH ₃	C ₆ H ₄ -4'-OH	A	60	DMF	>300	C ₁₆ H ₁₂ N ₄ O ₂	1690, 1580, 1280, 1160, 850, 760	3.84 (s, 3H, CH ₃); 6.85 (d, 2H, 3',5'-H); 7.35–7.72 (m, 3H, Ar-H); 8.05 (d, 2H, 2',6'-H); 8.43 (dd, 1H, 6-H); 9.74 (s, 1H, OH)	292 (60, M ⁺); 264 (25); 144 (82); 118 (100)
21	CH ₃	C ₆ H ₃ -3',4'-(OH) ₂		67	DMF/H ₂ O	282–284	C ₁₆ H ₁₂ N ₄ O ₃	3500, 1680, 1560, 1460, 1260, 750	3.86 (s, 3H, CH ₃); 6.74–7.73 (m, 6H, Ar-H); 8.46 (dd, 1H, 6-H); 9.01 (bs, 2H, 3',4'-OH)	308 (76, M ⁺); 280 (29); 144 (93); 118 (100)
22	CH ₃	thien-3-yl	A	80	DMF	225–226	C ₁₄ H ₁₀ N ₄ OS	1690, 1580, 1460, 1220, 810, 750	3.87 (s, 3H, CH ₃); 7.30–7.93 (m, 6H, Ar-H); 8.47 (dd, 1H, 6-H)	282 (100, M ⁺); 254 (25); 144 (59); 118 (90)
23	C ₆ H ₅	C ₆ H ₅		40	EtOH	228–230	C ₂₁ H ₁₄ N ₄ O	1670, 1580, 1450, 760	7.43–7.82 (m, 11H, Ar-H); 8.20–8.24 (m, 2H, Ar-H); 8.62 (dd, 1H, 5-H)	338 (22, M ⁺); 206 (81); 77 (100)
24	C ₆ H ₅	fur-2-yl		31	EtOH	248–250	C ₁₉ H ₁₂ N ₄ O ₂	1670, 1580, 1420, 1140, 760	6.72 (m, 1H, 4'-H); 7.43–7.47 (m, 9H, Ar-H); 7.92 (d, 1H, 5'-H); 8.61 (dd, 1H, 6-H)	328 (34, M ⁺); 206 (34); 93 (100); 77 (80)
25	CH ₂ C ₆ H ₅	C ₆ H ₅	A	70	DMF	180–181	C ₂₂ H ₁₆ N ₄ O	1700, 1560, 1380, 1280, 1150, 750	5.66 (s, 2H, CH ₂); 7.27–8.22 (m, 13H, Ar-H); 8.50 (dd, 1H, 6-H)	352 (43, M ⁺); 324 (2); 220 (19); 91 (100)
26	CH ₂ C ₆ H ₅	C ₆ H ₄ -4'-OH	A	36	DMF	287–289	C ₂₂ H ₁₆ N ₄ O ₂	1660, 1600, 1560, 1280, 1210, 760	5.62 (s, 2H, CH ₂); 6.86 (d, 2H, 3',5'-H); 7.27–7.68 (m, 8H, Ar-H); 8.09 (d, 2H, 2',6'-H); 8.48 (dd, 1H, 6H); 9.76 (s, 1H, OH, exch. with D ₂ O)	368 (44, M ⁺); 340 (2); 220 (16); 91 (100)
27	CH ₂ C ₆ H ₅	fur-2-yl	A	25	DMF/H ₂ O	233–235	C ₂₀ H ₁₄ N ₄ O ₂	1680, 1570, 1310, 1020, 750	5.64 (s, 2H, CH ₂); 6.59–6.65 (m, 1H, 4'-H); 7.23–7.60 (m, 9H, Ar-H); 7.78 (d, 1H, 5'-H); 8.47 (dd, 1H, Ar-H)	342 (7, M ⁺); 220 (4); 91 (100)
28	CH ₂ C ₆ H ₅	thien-3-yl	A	76	DMF	210–212	C ₂₀ H ₁₄ N ₄ OS	1680, 1450, 1140, 800, 750	5.64 (s, 2H, CH ₂); 7.24–7.63 (m, 10H, Ar-H); 7.92 (dd, 1H, Ar-H); 8.50 (dd, 1H, 6-H)	358 (36, M ⁺); 330 (1); 220 (12); 91 (100)

^a Elemental analyses for C, H, N were within ±0.4% of the calculated values. ^b Literature ref 82.

ethanol at 0 °C, then refluxing the reaction mixture for 4 h; (B) by refluxing the acids for 1 h in glacial acetic acid.

In the reaction of compound **30** with the appropriate glyoxylic acids in refluxing ethanol, it was not possible to isolate the intermediate hydrazone derivatives, but the target products **23** and **24** were directly obtained (Scheme 1, Table 3).

The results of the radioligand binding assays performed on the new ATBI compounds (Table 1) revealed

that a phenyl ring in place of the methyl at the N10-position increases affinity by 2.6–3.5-fold (compare **23** and **24** vs **12** and **16**), compound **23** being the most potent of all the investigated ATBIs with a *K_i* value of 18 nM. In contrast, the insertion of the benzyl at the N10-position lowered affinity by 1.2–5.7-fold (compare **25–28** vs **12**, **20**, **16**, and **22**). These data argue for a hydrophobic interaction at the L1 site which is sensitive to steric effects. The phenyl ring of the benzyl moiety is oriented to a large extent out of the plane of the

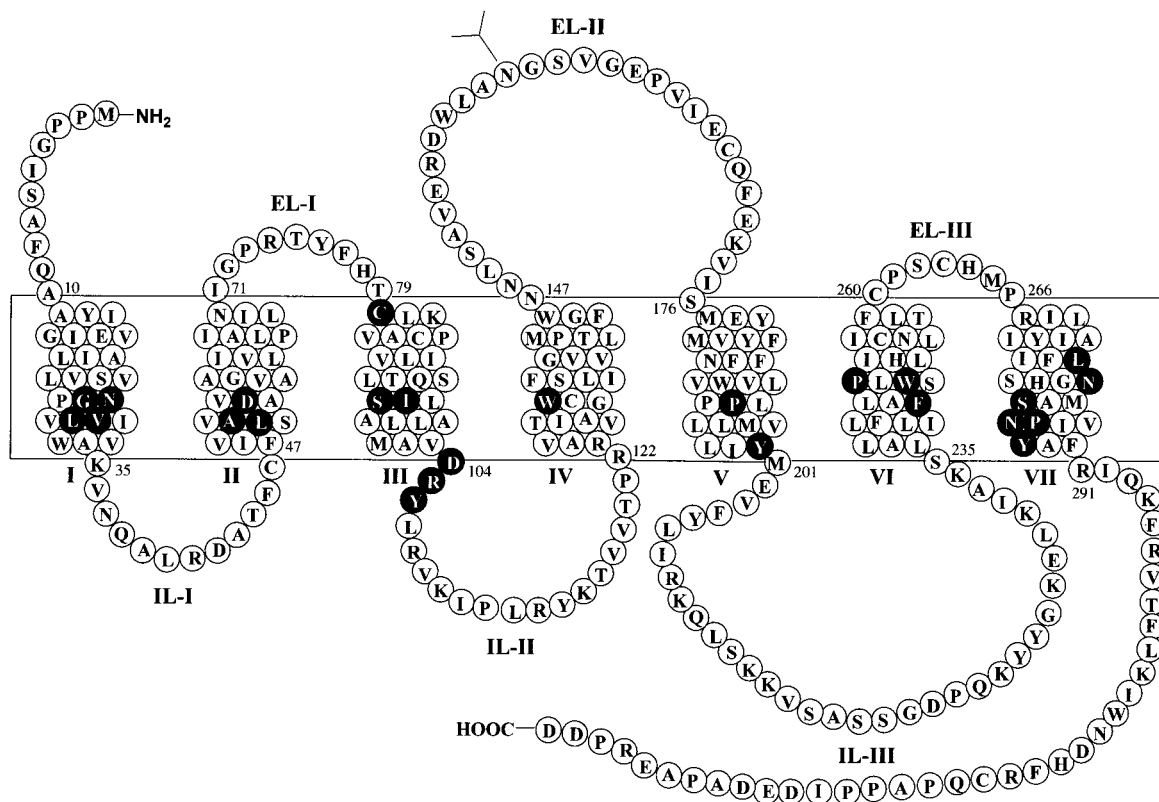


Figure 3. Serpentine model of bovine A₁AR sequence. The black lines represent the boundaries of the membrane. Filled circles indicate the residues highly conserved among the GPCRs superfamily. The TM helices are denoted by roman numerals. The arabic numbers indicate the position of the residues inside the TM domain. Glycosylation site on the EL-II is also shown. IL = intracellular loop and EL = extracellular loop.

Table 4. Intrinsic Activity of ATBI Derivatives **3**, **12**, **23**, and **25** to A₁AR Expressed as GTP Shift

no.	K_i A ₁ ^a -GTP (nM)	K_i A ₁ ^a +GTP (nM)	GTP shift
R-PIA	4.2 ± 0.3	19.9 ± 1.4	4.7
3	141.2 ± 13	197.3 ± 16	1.3
12	93.1 ± 7.3	119.2 ± 10	1.3
23	24.7 ± 2.2	25.0 ± 2.3	1.0
25	240 ± 19	184 ± 15	0.8

^a Displacement of [³H]DPCPX from bovine cortical membranes in the absence and in the presence of 1mM GTP. Values are taken from four experiments, expressed as means ± SEM.

molecular mainframe and probably, in such an arrangement, it cannot fit properly into the L1 site.

At the A₁AR, the selected compounds **3**, **12**, **23**, and **25** displayed no significant GTP shift, suggesting that they elicited an antagonist profile. In contrast, the standard agonist R-PIA exhibited a larger GTP shift value of 4.7 (Table 4).

Construction of a Model of the Bovine A₁AR and Docking Simulations. Models of the A₁AR complexed with antagonists were developed to aid the interpretation of the SARs in the class of A₁ antagonists and, perspective, to design new ATBI derivatives and analogues.

A bacteriorhodopsin-based model for the canine A₁AR has been proposed by IJzerman and co-workers.²¹ However, given the drawbacks of choosing bacteriorhodopsin as a template,³⁴ we constructed a model of bovine A₁AR³⁵ using as a template the frog rhodopsin,^{36,37} a membrane protein belonging to the G-protein coupled receptors (GPCRs) superfamily.

Table 5. Geometries of the Interhelical Hydrogen Bonds in the Model of Bovine A₁ Adenosine Receptor

residue ^a	acceptor ^b (A)	residue ^a	donor ^b (D)	H-A ^c (Å)	D-H-A ^d (deg)
Ile15	O	His278	N ^δ H	2.2	170
Ser23	O	<u>Asn27</u>	N ^{δ2} H	2.2	155
Cys46	O	Ser50	O ^γ H	2.1	147
Asp55	O ^{δ1}	Asn27	N ^{δ1} H	2.3	150
Asp55	O ^{δ2}	Asn284	N ^{δ1} H	2.3	153
Asp104	O ^{δ2}	<u>Arg291</u>	N ^{η2} H ₂	2.3	155
Val137	O	<u>Thr141</u>	O ^γ H	2.0	177
Val138	O	<u>Gln92</u>	N ^{ε2} H	2.3	130
Glu178	O ^{ε1}	Tyr182	O ^γ H	2.1	151
Trp247	O	His251	N ^δ H	2.1	140
Leu253	O	<u>Thr257</u>	O ^γ H	1.9	167
Ala273	O	<u>Ser277</u>	O ^γ H	2.3	164
Asn284	O ^{δ1}	Ser94	O ^γ H	2.3	139
Asn284	O ^{δ1}	Asn280	N ^{δ2} H	2.4	138

^a Residues highly conserved in GPCRs are in bold. Residues specifically conserved in ARs subtypes are underlined. ^b Atom names of the amino acids are based on IUPAC nomenclature.⁸³ ^c H-A is the hydrogen-acceptor distance. ^d D-H-A is the donor-acceptor angle.

The computational procedures described in the Experimental Section resulted in a protein structure quite stable during the molecular dynamics (MD) simulation and deviating from the initial geometry by a root-mean-square (rms) distance of 1.5 Å about the backbone atoms. Figure 3 is a serpentine scheme of bovine A₁AR sequence. Examination of the receptor model reveals two clusters of polar and aromatic side chains that form extensive networks of interhelical contacts. Table 5 details the interhelical hydrogen bonds computed over the minimized average structure of the protein. In this table, residues highly conserved in GPCRs and residues

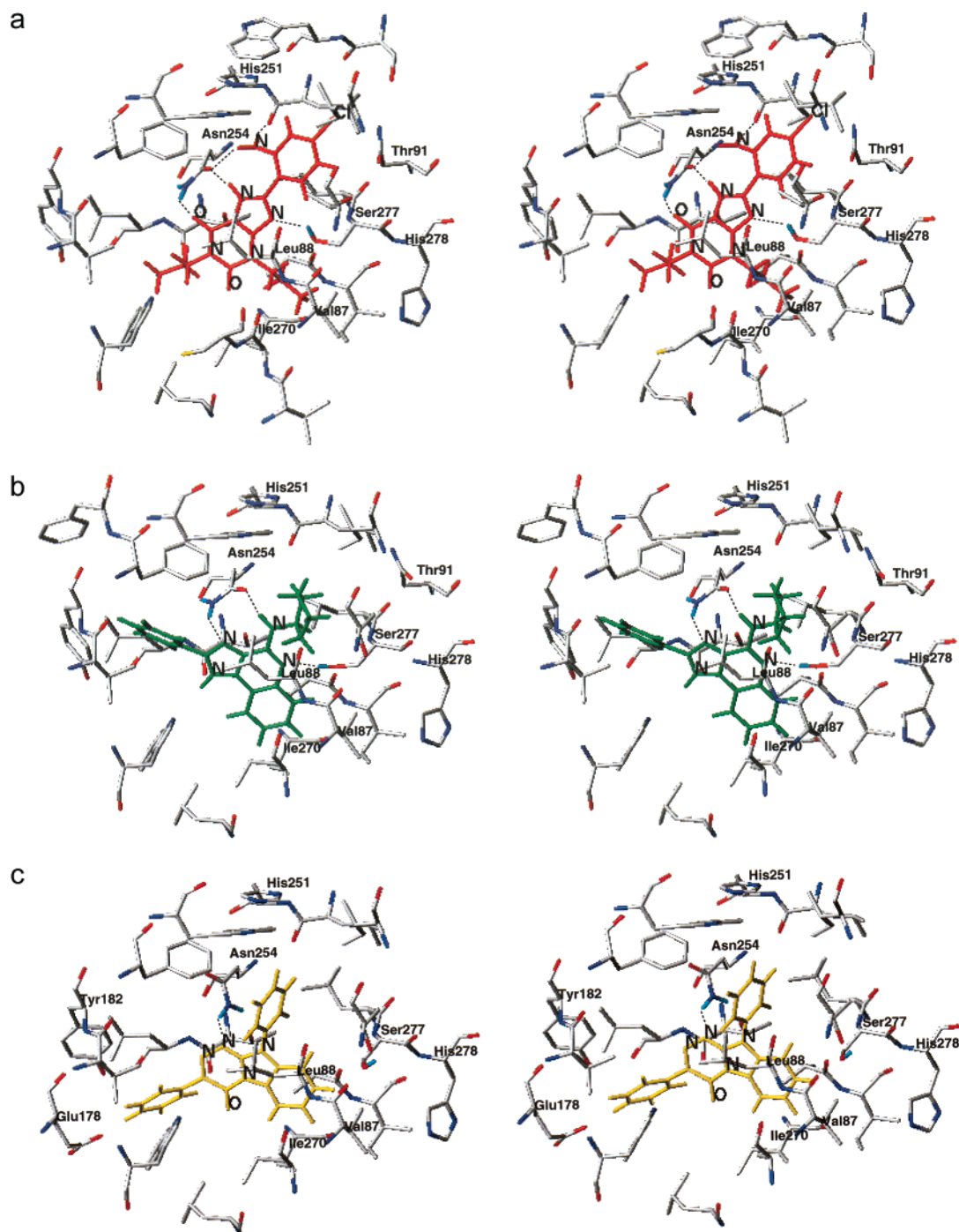


Figure 4. Theoretical models of the A₁AR binding site complexed with compounds **III** (a), **VII** (b), and **23** (c). Only amino acids located within 5 Å from any atom of the bound ligand are displayed. Dotted lines highlight ligand/receptor hydrogen bonds.

specifically conserved in ARs are in bold and are underlined, respectively. Two hydrogen bonds received by Asp55 (TMII) from Asn27 (TMI) and Asn284 (TMVII), whose role in maintaining the structural organization and functional integrity of the protein has been experimentally ascertained,^{38–40} were initially imposed through specific constraints and found to persist throughout the MD simulation. The seven-helical bundle is also stabilized by a network of π -stacking interactions⁴¹ involving a number of residues highly conserved in GPCRs (Phe243 and Trp247 in helix VI along with Tyr200 in helix V) and peculiar of the ARs family (Phe185 and Trp188 in helix V together with His251 in helix VI). Our model is also in agreement with the substituted cysteine

accessibility studies of Javitch et al.,^{42–45} who placed various conserved residues and residues accessible to polar Cys probes on helices III, V, VI, and VII inside the core of the transmembrane bundle.

Compound **VII** was docked into the model of A₁AR using the automated DOCK 3.5 suite of programs.^{46–49} This ligand was selected as representative of A₁AR antagonists primarily because, compared with the structures reported in Figure 1 and the ATBI derivative **23**, it possesses low flexibility and all the six hypothesized pharmacophoric features (see Figure 2). Among the “best” orientations proposed by DOCK, we chose that with the HN-CC-N substructure of **VII** facing the Asn247 side chain so as to make two hydrogen bonds.

Table 6. Residues of the Bovine A₁ Adenosine Receptor Binding Cleft and Their Relationship with the Pharmacophoric Binding Sites^a

site ^b	residues ^c
L1	Val87 (III), Leu88 (III), Thr91 (III), Ile95 (III), Phe185 (V), Trp188 (V), Trp247 (VI), Leu250 (VI), His251 (VI), Leu276 (VII), Asn280 (VII)
L2	Leu81 (III), Leu88 (III), Trp146 (IV), Val181 (V), Tyr182 (V), Phe185 (V), Thr257 (VI), <u>Leu258</u> (VI)
L3	Leu81 (III), <u>Ala84</u> (III), Val87 (III), Leu88 (III), <u>Ile270</u> (VII), <u>Ala273</u> (VII), Ile274 (VII), Leu276 (VII)
HB1/HB2	Asn254 (VI)
HB3	Ser277 (VII)

^a Amino acids of the binding site are those located within 5 Å from any atom of the docked ligands **III**, **VII**, and **23**. ^b These sites are illustrated in Figure 2. ^c A₁AR specific residues are underlined. The transmembrane domain is given in parentheses.

This type of double hydrogen bond between an Asn residue and an adenine derivative is a motif characterizing several ligand/protein complexes⁵⁰ filed in the Brookhaven Protein Data Bank.⁵¹

The geometry of the **VII**/A₁AR complex was then optimized by MD and energy minimization (EM) cycles. Compounds **III**⁵² and **23** were initially placed into the receptor binding site by fitting them on the docked conformation of **VII** according to the pharmacophoric alignment shown in Figure 2. The resulting complexes were then submitted to geometry refinement protocols based on MD and EM calculations.

Figure 4 illustrates the docking models developed for compounds **III**, **VII**, and **23**. Table 6 summarizes the amino acids located within 5 Å from the bound ligands and their relationship with the pharmacophoric binding sites HB1, HB2, HB3, L1, L2, and L3 (Figure 2). Site-directed mutagenesis experiments have underscored the importance of several residues listed in Table 6 in favoring the binding of different A₁AR antagonists: Val87, Leu88, Thr91,⁵³ Ser277,^{54,55} Ile270,⁵⁵ and His251.⁵⁶ The Asn247 side chain corresponds to the hydrogen bond acceptor and donor sites HB1 and HB2, while Ser277 might represent the HB3 donor site. A hydrogen bond with Ser277 does not seem mandatory for high affinity since this interaction is missing in the complex of the highly potent ligand **23**. At the end of the geometry refinement calculations on the **23**/A₁AR complex, we found that the N1 nitrogen of **23** receives a hydrogen bond from the Asn247 side chain (Figure 4c) whereas it was the vicinal N2 nitrogen to be initially considered as a pharmacophoric element in **12** (Figures 1 and 2).

The L2 site, assumed to be relatively small as inferred from the SARs in the ATBI series, is located at the binding site entrance of the receptor. It is likely that the steric borders of the L2 region are atoms of the extracellular loops II and III not included in our model for obvious reasons. It is tempting to speculate that the side chains of Glu178 and Tyr182 in helix V, surrounding the pendant phenyl moiety of the docked ligand, might receive hydrogen bonds from the *meta* and *para* hydroxyls which, as already stated, are the only substituents tolerated. In the previous paragraph, we hypothesized that the lower affinity of the N10-benzyl compared with the N10-phenyl ATBI derivatives could be related to a hydrophobic interaction at the L1 site strongly influenced by shape-dependent effects. Figure

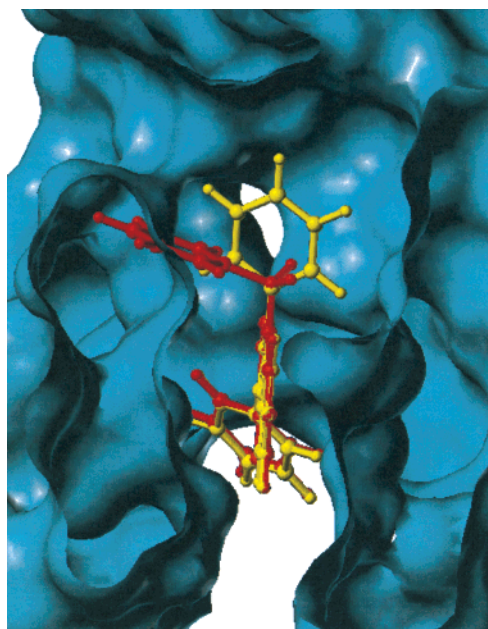


Figure 5. Overlay of the N10-benzyl derivative **25** (red) on the docked N10-phenyl derivative **23** (yellow). The A₁AR binding site is portrayed as a solvent accessible surface and is clipped to display the interaction between the N10-substituents and the L1 lipophilic pocket.

5 illustrates a Connolly surface of the receptor hosting the docked compound **23** (N10-phenyl) together with the structure of the **25** (N10-benzyl) overlayed about their common skeleton. The excellent degree of steric complementarity between the N10-phenyl and the L1 pocket can be appreciated in contrast with the steric conflict between the N10-benzyl group and a part of the receptor⁵⁷ probably requiring energetically expensive conformational changes in one or both partners of the **25**/A₁AR complex. Despite the many limitations of pharmacophore and docking models (e.g., the possibility of alternate and multiple binding modes^{58,59}), our model of A₁AR complexed with **23** rationalizes the SARs in the ATBI series and will be employed to guide further lead optimization projects.

Conclusions

We have disclosed a series of 3-aryltriazinobenzimidazolones (ATBIs) as a novel class of A₁AR antagonists generally selective over A_{2A} and A₃ARs. Attempts to improve A₁AR affinity in the ATBIs, guided by an overlay of the lead compound **12** (*K_i* = 63 nM) on some well-known A₁AR antagonists, yielded compound **23** characterized by a *K_i* of 18 nM. Finally, we built a model of the bovine A₁AR to rationalize the SARs of ATBIs and to facilitate, perspective, the design of new analogues.

Experimental Section

Chemistry. Melting points were determined using a Reichert Köfeler hot-stage apparatus and are uncorrected. Infrared spectra were obtained on a PYE/UNICAM mod. PU 9561 spectrophotometer in Nujol mulls. Nuclear magnetic resonance spectra were recorded in DMSO-*d*₆ solutions with a Varian Gemini 200 or a Varian CFT-20 spectrometer using tetramethylsilane (TMS) as an internal standard. Mass spectra were obtained on a Hewlett-Packard 5988 A spectrometer using a direct injection probe and an electron beam energy of 70 eV. Magnesium sulfate was always used as the drying

agent. Evaporations were made in vacuo (rotating evaporator). Analytical TLC was carried out on Merck 0.2 mm precoated silica gel aluminum sheets (60 F-254). Silica gel 60 (230–400 mesh) was used for flash column chromatography. Elemental analyses were performed by our Analytical Laboratory and agreed with theoretical values within $\pm 0.4\%$.

Besides the commercially available starting materials, 4-hydroxyphenyl glyoxylic acid⁶⁰ and 3-thienylglyoxylic acid⁶¹ were prepared in accordance with the reported methods.

3-Substituted 1-Methyl (18–20,22) and 3-Substituted 1-Benzyl[1,2,4]triazino[4,3-*a*]benzimidazol-4(10*H*)-ones (25–28). A solution of 1-methyl- (29) or 1-benzyl-2-hydrazinobenzimidazole (31) (4 mmol) and the appropriate glyoxylic acid (4.4 mmol) in 10 mL of ethanol was refluxed for 2 h. The mixture was cooled, and the precipitate was collected to give the 2-substituted 2-(benzimidazol-2-ylhydrazono)acetic acids 32–35 and 36–39 which were purified by suspension in hot methanol (Table 2).

They can be cyclized by means of the following methods.

Method A. A suspension of the acid derivatives 34, 35 and 36–39 (2 mmol) in 5 mL of absolute ethanol, at 0 °C, was saturated with anhydrous HCl and then refluxed for 4–7 h, and the reaction was monitored by TLC analysis. The reaction mixture was evaporated to dryness, and the solid residue was treated with saturated sodium hydrogencarbonate aqueous solution. The crude product obtained was purified by recrystallization from the appropriate solvent (Table 3).

Method B. A suspension of the acids 32, 33 (2 mmol) in 20 mL of glacial acetic acid was refluxed for 1 h. The solution obtained was evaporated to dryness, and the oily residue was filtered on a silica gel chromatographic column ($h = 4$ cm; $\phi = 2.5$ cm; eluting system = toluene:chloroform = 1:1). The crude solid product obtained was purified by recrystallization from the appropriate solvent (Table 3).

3-Substituted 1-Phenyl[1,2,4]triazino[4,3-*a*]benzimidazol-4(10*H*)-ones (23, 24). A solution of 30 (4 mmol) and the appropriate glyoxylic acid (4.4 mmol) in 10 mL of absolute ethanol was refluxed for 3–5 h (TLC analysis). After cooling, the precipitate that formed was collected and purified by recrystallization from the appropriate solvent (Table 3).

3-(3',4'-Dihydroxyphenyl)-1-methyl[1,2,4]triazino[4,3-*a*]benzimidazol-4(10*H*)-one (21). A solution of boron tribromide (6 mmol) in 1 mL of anhydrous dichloromethane was added dropwise, at -10 °C, under stirring and in a nitrogen atmosphere, to a suspension of the dimethoxy derivative 15¹ (0.9 mmol) in 8 mL of the same solvent. Stirring was continued for 30 min at -10 °C and for 1 h at room temperature. The reaction mixture was carefully added dropwise to 5 mL of methanol at -10 °C. The suspension obtained was evaporated to dryness, and the solid residue was treated with saturated sodium hydrogen carbonate aqueous solution. The crude product 21 was collected and purified by recrystallization (Table 3).

Biological Methods. Materials. [³H]-(R)-PIA (25 Ci/mmol) was purchased from Amersham Corp. (Little Chalfont, Buckinghamshire, U.K.), while [³H]CHA, [¹²⁵I]AB-MECA, and [³H]CGS 21680 were obtained from DuPont-NEN (Boston, MA). DPCPX was purchased from RBI (Natick, MA). Adenosine deaminase was from Sigma Chemical Co. (St. Louis, MO). All other reagents were from standard commercial sources and of the highest commercially available grade.

Receptor Binding Assays. A₁ and A_{2A} Receptor Binding. Displacement of [³H]CHA (31 Ci/mmol) from A₁AR in bovine cortical membranes and of [³H]CGS 21680 (42.1 Ci/mmol) from A_{2A}AR in bovine striatal membranes was performed as described.⁶² Adenosine A₁ receptor affinities with [³H]DPCPX as radioligand were determined according to Pirovano et al.⁶³ Measurements with [³H]DPCPX were performed in the presence and in the absence of 1 mM GTP.

A₃AR Binding. [¹²⁵I]AB-MECA binding to A₃AR in bovine cortical membranes was performed in 50 mM Tris, 10 mM MgCl₂, and 1 mM EDTA buffer (pH 7.4) containing 0.2 mg of proteins and 2 U/mL adenosine deaminase and 20 nM DPCPX.²⁸ Incubations were carried out in duplicate for 90 min at 25 °C.

Nonspecific binding was determined in the presence of 50 μ M R-PIA and constituted approximately 30% of the total binding. Binding reaction was terminated by filtration through a Whatman GF/C filter, washing three times with 5 mL of ice-cold buffer.

All compounds were routinely dissolved in DMSO and diluted with assay buffer to the final concentration, where the amount of DMSO never exceeded 2%.

At least six different concentrations spanning 3 orders of magnitude, adjusted appropriately for the IC₅₀ of each compound, were used. IC₅₀ values, computer-generated using a nonlinear regression formula on a computer program (GraphPad, San Diego, CA), were converted to K_i values, knowing the K_d values of radioligands in the different tissues and using the Cheng and Prusoff equation.⁶⁴ The dissociation constant (K_d) of [³H]CHA, [³H]CGS 21680, and [¹²⁵I]AB-MECA were 1.2, 14, and 1.02 nM, respectively.

Computational Procedures. A₁ Adenosine Receptor Model Building. All model building, energy minimizations, and molecular dynamics calculations were carried out using SYBYL 6.2⁶⁵ and AMBER 4.1^{66,67} modeling packages, respectively. All manipulations were performed on a Silicon Graphics R10000 workstation.

The structural model of the bovine A₁AR has been derived from electron cryomicroscopy data³⁶ and the C α coordinate template provided by Baldwin et al.³⁷ This template was generated from rhodopsin projection data in combination with a sequence analysis of 493 GPCRs, including ARs.³⁷ The seven TM helical domains were identified with the aid of Kyte–Doolittle hydrophobicity⁶⁸ and E_{mini} ⁶⁸ surface probability parameters. The length of the helices was determined by considering the minimum length in the lipid bilayer, as defined by Baldwin, with subsequent addition of residues at the extracellular and intracellular limits based on sequence analysis of this region. Individual TM helical segments were built as ideal helices (using ϕ – ψ angles of -63.0° and -41.6°) with side chains placed in prevalent rotamers and representative proline kink geometries. Each helix was capped with an acetyl group and an *N*-methyl group at the N-terminus and at the C-terminus, respectively. These structures were then grouped together to form a helical bundle matching the overall characteristics of the electron density map of rhodopsin.

The relative orientations and interactions between the helices were adjusted based on incorporated structural inferences from available experimental data, such as mutation and ligand binding studies,^{69–71} cysteine scanning data,^{42–45} and site-directed mutation experiments.^{38–40} Because earlier work showed that polarity conserved positions cluster together in the cores of proteins to create conserved hydrogen-bonding interactions,⁷² we refined the model by applying the additional hydrogen-bonding constraints between the conserved polar residues Asn27, Asp55, and Asn284 in accordance with data from site-directed mutagenesis.^{38–40}

The helical bundle was subjected to energy-minimization using the SANDER module of the AMBER suite of programs^{66,67} until the rms value of the conjugate gradient was 0.001 kcal/mol/Å. An energy penalty force constant of 5 kcal/Å²/mol to the protein backbone atoms was applied throughout these calculations. The resultant model was further used as the starting point for a series of short MD simulations at 300 K, during which the positional constraints on the protein backbone atoms were gradually released from 5 to 0.05 kcal/Å²/mol. A 1 fs time step was used along with a nonbonded cutoff of 8 Å, and the nonbonded pair list updated every 25 fs. The temperature of the system was maintained at 300 K using the Berendsen algorithm⁷³ with a 0.2 ps coupling constant.

The structural quality of the model was also evaluated using the PROCHECK 3.4.4 program,⁷⁴ which examines the values of the dihedral angles of the protein backbone and side chains. Analysis of main chain torsion angles showed that 98% of the residues are located in the most favored helical regions, the remaining 2% occurring in the additional allowed helical regions of the Ramachandran plot. Side chain χ_1 and χ_2

dihedrals were determined to be in their most favorable regions without steric conflicts.

Pharmacophore-Based Alignment and Docking Simulations. The core structures of the ligands were retrieved from the Cambridge Structural Database (CSD)⁷⁵ and modified whenever necessary using the SYBYL fragment library. The resulting structures were fully optimized using the semi-empirical quantum mechanics method AM1⁷⁶ as implemented in the MOPAC 6.0 program⁷⁷ (keywords: PREC, GNORM = 0.01, EF, MMOK). Molecular graphics, rms fit, and calculations of ring centroids were also carried out using SYBYL.

The DOCK 3.5 suite of programs^{46–49} was used for automated docking simulations of compound **VII** to the model-built TM domain of the A₁AR. DOCK identifies specific orientations of a given ligand which are complementary to a targeted surface area. In brief, DOCK first generates a negative image of the ligand binding site as a set of overlapping spheres whose centers become the potential locations for ligand atoms. To rank each potential binding mode, a precalculated contact scoring grid (based on distances between potential ligand and target area atoms) and a force field scoring grid (based on steric and electrostatic interaction energies) are generated. The resulting output file for each screen, based on distance or force field grids, contains the highest scoring orientations ranked in order of their scores.

In absence of any information concerning the 3D structure of the loops of GPCRs, these domains were not considered in our study. On the other hand, site-directed mutagenesis experiments and studies on chimeric A₁/A₂/A₃ARs^{53–56} strongly suggest that ligand/receptor binding occurs at the TM domain of these receptors. A molecular surface representation of all residues within 6 Å of the putative ligand binding pocket of the A₁AR TM helices was obtained by using the MS program^{78,79} and a probe of 1.4 Å radius. The surface points and their associated normals were adopted using the module SPHGEN⁸⁰ to fill the active site with a set of overlapping spheres, as descriptors of the volume available to the ligand. A cutoff distance of 4.5 Å for "good-contacts" with the receptor was applied.^{46–49} The specific sphere cluster utilized was a manually edited cluster comprising 42 individual spheres, which satisfactorily covered the target area. The module CHEMGRID⁴⁶ was used to precompute and save in a grid file the information necessary for force field scoring. The molecules were docked into the receptor binding pocket using the single mode option in DOCK, and the quality of the ligand binding was evaluated by a force field scoring function. Each orientation of each ligand was filtered for steric fit through a DISTMAP grid⁴⁸ with polar and nonpolar contact limits of 1.3 and 1.8 Å, respectively.

The putative pharmacophore-based conformation of **VII** was directly docked. Out of the 3057 orientations obtained, 75 were within 5 kcal/mol of the best orientation based on the scoring function. Inspection of the docked structures revealed that the best and many of the top scoring orientations placed the HN-CC-N substructure of **VII** facing the Asn247 side chain so as to make two hydrogen bonds. From this cluster of structures, we selected one (force field score –22.1 kcal/mol, 2 kcal/mol above the top scoring orientation) in which the nitrogen closest to the pendant phenyl ring made a hydrogen bond with the Ser277 side chain.

Refinement of the ligand/receptor bound complex was achieved by in vacuo energy minimization with the SANDER module of AMBER 4.1 (50 000 steps; distance dependent dielectric function of $\epsilon = 4r$), applying an energy penalty force constant of 5 kcal/mol on the protein backbone atoms. The geometry-optimized structures were then used as the starting point for subsequent 200 ps MD simulation, during which the protein backbone atoms were constrained as done in the previous step. The simulations employed the Cornell force field,⁸¹ as implemented in the AMBER 4.1 suite of programs.^{66,67} The additional parameters required for the ligands were derived by analogy to existing parameters. Partial atomic charges for the ligands were imported from the output files of AM1 full geometry optimizations. A time step of 1 fs and a

nonbonded pairlist updated every 25 fs were used for the MD simulations. The temperature was maintained at 300 K using the Berendsen algorithm⁷³ with a 0.2 ps coupling constant. Four snapshots, extracted each 25 ps from the last 100 ps MD simulation, were very similar in terms of rms deviation. An average structure was calculated from the last 100 ps trajectory and energy-minimized using the steepest descent and conjugate gradient methods available within the SANDER module of AMBER as specified above.

Connolly solvent accessible surfaces of the A₁AR binding site (based on a probe radius of 1.4 Å) were generated using the SYBYL/SURFACE routine run under default settings.

Acknowledgment. This work was supported by grants from the Ministry of University and Scientific and Technological Research (MURST).

Note Added in Proof: After this manuscript was submitted, a paper was published disclosing the crystal structure of rhodopsin solved diffractometrically at 2.8 Å resolution (Palczewski, K.; Kumasaka, T.; Hori, T.; Behnke, C. A.; Motoshima, H.; Fox, B. A.; Le Trong, I.; Teller, D. C.; Okada, T.; Stenkamp, R. E.; Yamamoto, M.; Miyano, M. Crystal Structure of Rhodopsin: A G Protein-Coupled Receptor. *Science* **2000**, *289*, 739–745). A comparison of our A₁AR model with this crystal structure revealed slight differences in the orientations of the transmembrane helices and a satisfying overlap about the residues of the putative adenosine binding pocket.

References

- (1) Primofiore, G.; Da Settimo, F.; Taliani, S.; Marini, A. M.; La Motta, C.; Novellino, E.; Greco, G.; Gesi, M.; Trincavelli, L.; Martini, C. 3-Aryl[1,2,4]triazino[4,3-a]benzimidazol-4(10H)-ones: Tricyclic Heteroaromatic Derivatives as a New Class of Benzodiazepine Receptor Ligands. *J. Med. Chem.* **2000**, *43*, 96–102.
- (2) Suzuki, F.; Shimada, J.; Nonaka, H.; Ishii, A.; Shiozaki, S.; Ichikawa, S.; Ono, E. 7,8-Dihydro-8-ethyl-2-(3-noradamantyl)-4-propyl-1H-imidazo[2,1-f]purin-5(4H)-one: A Potent and Water-Soluble Adenosine A₁ Antagonist. *J. Med. Chem.* **1992**, *35*, 3578–3581.
- (3) Shimada, J.; Suzuki, F.; Nonaka, H.; Ishii, A. Polycycloalkyl-1,3-dipropylxanthines as Potent and Selective Antagonists for A₁-Adenosine Receptor. *J. Med. Chem.* **1992**, *35*, 924–930.
- (4) Suzuki, F.; Shimada, J.; Mizumoto, H.; Karasawa, A.; Kubo, K.; Nonaka, H.; Ishii, A.; Kawakita, T. Adenosine A₁ Antagonists 2. Structure–Activity Relationships on Diuretic Activities and Protective Effects Against acute Renal Failure. *J. Med. Chem.* **1992**, *35*, 3066–3075.
- (5) Bruns, R. F.; Lu, G. H.; Pugsley, T. A Characterization of the A₂ Adenosine Receptor Labeled by [³H]NECA in Rat Striatal Membranes. *Mol. Pharmacol.* **1986**, *29*, 331–346.
- (6) Hamilton, H. W.; Ortwine, D. F.; Worth, D. F.; Bristol, J. A. Synthesis and Structure–Activity Relationships of Pyrazolo[4,3-d]pyrimidin-7-one as Adenosine Receptor Antagonists. *J. Med. Chem.* **1987**, *30*, 91–96.
- (7) Sarges, R.; Howard, H. R.; Browne, R. G.; Lebel, L. A.; Seymour, P. A.; Koe, B. K. 4-Amino[1,2,4]triazolo[4,3-a]quinoxalines. A Novel Class of Potent Adenosine Receptor Antagonists and Potential Rapid-Onset antidepressants. *J. Med. Chem.* **1990**, *33*, 2240–2254.
- (8) Francis, J. E.; Cash, W. D.; Psychoyos, S.; Ghai, G.; Wenk, P.; Friedmann, R. C.; Atkins, C.; Warren, V.; Furness, P.; Hyun, J. L.; Stone, G. A.; Desai, M.; Williams, M. Structure–Activity Profile of a series of Novel Triazoloquinazoline Adenosine Antagonists. *J. Med. Chem.* **1988**, *31*, 1014–1020.
- (9) van Galen, P. J. M.; Nissen, P.; Van Wijngaarden, I.; IJzerman, A. P.; Soudijn, W. 1H-Imidazo[4,5-c]quinolin-4-amine: Novel Non-Xanthine Adenosine Antagonists. *J. Med. Chem.* **1991**, *34*, 1202–1206.
- (10) Müller, C. E.; Hide, I.; Daly, J. W.; Rothenhäusler, K.; Eger, K. 7-deaza-2-phenyladenines: Structure–Activity Relationships of Potent A₁ Selective Adenosine Receptor Antagonists. *J. Med. Chem.* **1990**, *33*, 2822–2828.
- (11) Jacobson, K. A.; van Galen, P. J. M.; Williams, M. Adenosine Receptors-Pharmacology, Structure–Activity Relationships, and Therapeutic Potential. *J. Med. Chem.* **1992**, *35*, 407–422.
- (12) Von Lubitz, D. K. J. E.; Jacobson, K. A. Behavioral Effects of Adenosine Receptor Stimulation. In *Adenosine and Adenine Nucleotides: From Molecular Biology to Integrative Physiology*; Belardinelli, L., Pelleg, A., Eds.; Kluwer: Norwell, 1995; pp 489–498.

- (13) Collis, M. G.; Hourani, S. M. O. Adenosine Receptor Subtypes. *Trends Pharmacol. Sci.* **1993**, *14*, 360–366.
- (14) Poulsen, S.-A.; Quinn, R. J. Adenosine Receptors for Future Drugs. *Bioorg. Med. Chem.* **1998**, *6*, 619–641.
- (15) Kim, H. O.; Ji, X. D.; Melman, N.; Olah, M. E.; Stiles, G. L.; Jacobson, K. A. Structure–Activity Relationships of 1,3-Dialkyl-xanthine Derivatives at Rat A₃ Adenosine Receptors. *J. Med. Chem.* **1994**, *37*, 3373–3382.
- (16) van Galen, P. J. M.; van Bergen, A. H.; Gallo-Rodriguez, C.; Olah, M. E.; IJzerman, A. P.; Stiles, G. L.; Jacobson, K. A. A Binding Site Model and Structure–Activity Relationships for the Rat A₃ Adenosine Receptor. *Mol. Pharmacol.* **1994**, *45*, 1101–1111.
- (17) Peet, N. P.; Lentz, N. L.; Meng, E. C.; Dudley, M. W.; Ogden, A. M. L.; Demeter, D. A.; Weintraub, H. J. R.; Bey, P. A Novel Synthesis of Xanthines: Support for a New Binding Mode for Xanthines with Respect to Adenosine at Adenosine Receptors. *J. Med. Chem.* **1990**, *33*, 3127–3130.
- (18) van Galen, P. J. M.; van Vlijmen, H. W. T.; IJzerman, A. P.; Soudijn, W. A Model for the Antagonist Binding Site on the Adenosine A₁ Receptor Based on Steric, Electrostatic, and Hydrophobic Properties. *J. Med. Chem.* **1990**, *33*, 1708–1713.
- (19) Quinn, R. J.; Dooley, M. J.; Escher, A.; Harden, F. A.; Jayasuriya, H. A Computer Generated Model of Adenosine Receptors Rationalising binding and Selectivity of Receptor Ligands. *Nucleosides Nucleotides* **1991**, *10*, 1121–1124.
- (20) Dooley, M. J.; Quinn, R. J. The Three Binding Domain Model of Adenosine Receptors: Molecular Modeling Aspects. *J. Med. Chem.* **1992**, *35*, 211–216.
- (21) IJzerman, A. P.; van Galen, P. J. M.; Jacobson, K. A. Molecular Modeling of Adenosine Receptors. I. The Ligand Binding Site on the A₁ Receptor. *Drug Des. Discovery* **1992**, *9*, 49–67.
- (22) Dudley, M. W.; Peet, N. P.; Demeter, D. A.; Weintraub, H. J. R.; Herschel, J. R.; IJzerman, A. P.; Nordvall, G.; van Galen, P. J. M.; Jacobson, K. A. Adenosine A₁ Receptor and Ligand Molecular Modeling. *Drug Des. Discovery* **1993**, *28*, 237–243.
- (23) IJzerman, A. P.; van der Wenden, E. M.; van Galen, P. J. M.; Jacobson, K. A. Molecular Modeling of Adenosine Receptors – The Ligand-Binding Site on the Rat Adenosine A_{2a} Receptor. *Eur. J. Pharmacol. Mol. Pharmacol. Sect.* **1994**, *268*, 95–104.
- (24) Dooley, M. J.; Kono, M.; Suzuki, F. Theoretical Structure–Activity Studies of Adenosine A₁ Ligands: Requirements for Receptor Affinity. *Bioorg. Med. Chem.* **1996**, *6*, 923–934.
- (25) The correspondences between Dooley's and our receptor binding sites are herein reported: N7 position/HB1, O⁶ oxygen/HB2, C8-position/L1, N1-position/L2, and N3-position/L3 (see Figure 7 in ref 15).
- (26) Bednyagina, N. P.; Postovskii, I. Ya. Benzazoles. 2-Hydrazino- and 2-Azidobenzimidazoles. *Zh. Obshchei Khim.* **1960**, *30*, 1431–1437; *Chem. Abstr.* **1961**, *55*, 1586h.
- (27) de Zwart, M.; Kourounakis, A.; Kooijman, H.; Spek, A. L.; Link, R.; von Frijtag Drabbe Künzel, J. K.; IJzerman, A. P. 5'-N-Substituted Carboxamidoadenosines as Agonists for Adenosine Receptors. *J. Med. Chem.* **1999**, *42*, 1384–1392.
- (28) Jacobson, K. A.; Nikodjivic, O.; Shi, D.; Gallo-Rodriguez, C.; Olah, M. E.; Stiles, G. L.; Daly, J. V. A Role for Central A₃-Adenosine Receptors Mediation of Behavioral Depressant Effects. *FEBS Lett.* **1993**, *336*, 57–60.
- (29) Tyurenkova, G. N.; Mudretsova, I. I.; Mertsalov, S. L.; Bednyagina, N. P. Synthesis, Structures and Tautomerism of Formazans Containing a 1-Arylbenzimidazol-2-yl Residue. *Khim. Geterotsikl. Soedin.* **1980**, *6*, 818–821; *Chem. Abstr.* **1980**, *93*, 203744p.
- (30) Robison, M. M. Chlorohydroxylation of Nitrogen Heterocycles with Phenylphosphonic Dichloride. *J. Am. Chem. Soc.* **1958**, *80*, 5481–5483.
- (31) Iemura, R.; Kawashima, T.; Ito, K.; Tsukamoto, G. Synthesis of 2-(4-Substituted-1-piperazinyl)benzimidazoles as H₁ Antihistaminic Agents. *J. Med. Chem.* **1986**, *29*, 1178–1183.
- (32) Clark, R. L.; Pessolano, A. A. Synthesis of Some Substituted Benzimidazolones. *J. Am. Chem. Soc.* **1958**, *80*, 1657–1662.
- (33) Eckert, H.; Forster, B. Triphosgene, a Crystalline Phosgene Substitute. *Angew. Chem., Int. Ed. Engl.* **1987**, *26*, 894–895.
- (34) Bikker, J. A.; Trumpp-Kallmeyer, S.; Humblet, C. G-Protein Coupled Receptors: Models, Mutagenesis, and Drug Design. *J. Med. Chem.* **1998**, *41*, 2911–2927.
- (35) The amino acid sequence of the bovine A₁AR was used in these studies to reflect the source of the binding affinity data consisting of bovine brain A₁AR membrane preparations.
- (36) Unger, V. M.; Hargrave, P. A.; Baldwin J. M.; Schertler, G. F. X. Arrangement of Rhodopsin Transmembrane Alpha Helices Obtained by Electron Cryo-microscopy. *Nature* **1997**, *389*, 203–206.
- (37) Baldwin, J. M.; Schertler, G. F. X.; Unger, V. M. An Alpha-carbon Template for the Transmembrane Helices in the Rhodopsin Family of G-protein-coupled Receptors. *J. Mol. Biol.* **1997**, *272*, 144–164.
- (38) Perlman, J. H.; Colson, A. O.; Wang, W.; Bence, K.; Osman R.; Gershengorn, M. C. Interactions Between Conserved Residues in Transmembrane Helices 1, 2, and 7 of the Tyrotropin-Releasing Hormone Receptor. *J. Biol. Chem.* **1997**, *272*, 11937–11942.
- (39) Sealfon, S. C.; Chi, L.; Eversole, B. J.; Rodic, V.; Zhang, D.; Ballesteros, J. A.; Weinstein, H. Related Contribution of Specific Helix 2 and 7 Residues to Conformational Activation of the Serotonin 5-HT_{2a} Receptor. *J. Biol. Chem.* **1995**, *270*, 16683–16688.
- (40) Zhou, W.; Flanagan, C. A.; Ballesteros, J.; Konvicka, K.; Davidson, J. S.; Weinstein, H.; Millar, R. P.; Sealfon, S. C. A Reciprocal Mutation Supports Helix 2 and Helix 7 Proximity in the Gonadotropin-releasing Hormone Receptor. *Mol. Pharmacol.* **1994**, *45*, 165–170.
- (41) Burley, S. K.; Petsko, G. A. Aromatic–Aromatic Interaction: a Mechanism of Protein Structure Stabilization. *Science* **1995**, *229*, 23–28.
- (42) Javitch, J. A.; Li, X.; Kaback, J.; Karlin, A. A Cysteine Residue in the Third Membrane-Spanning Segment of the Human D₂ Dopamine Receptor Is Exposed in the Binding-Site Crevise. *Proc. Natl. Acad. Sci. U.S.A.* **1994**, *91*, 10355–10359.
- (43) Javitch, J. A.; Fu, D. Y.; Chen, J. Y.; Karlin, A. Residues in the Fifth Membrane-Spanning Segment of the Dopamine D₂ Receptor Exposed in the Binding-Site Crevise. *Biochemistry* **1995**, *34*, 16433–16439.
- (44) Javitch, J. A.; Fu, D.; Liapakis, G.; Chen, J. Constitutive Activation of the 2 Adrenergic Receptor Alters the Orientation of its Sixth Membrane-Spanning Segment. *J. Biol. Chem.* **1997**, *272*, 18546–18549.
- (45) Fu, D.; Ballesteros, J. A.; Weinstein, H.; Chen, J.; Javitch, J. A. Residues in the Seventh Membrane-Spanning Segment of the Dopamine D₂ Receptor Accessible in the Binding-Site Crevise. *Biochemistry* **1996**, *35*, 11278–11285.
- (46) Meng, E. C.; Shoichet, B. K.; Kuntz, I. D. Automated Docking with Grid-Based Energy Evaluation. *J. Comput. Chem.* **1992**, *13*, 505–524.
- (47) Meng, E. C.; Gschwend, D. A.; Blaney, J. M.; Kuntz, I. D. Orientational Sampling and Rigid-Body Minimization in Molecular Docking. *Proteins: Struct., Funct., Genet.* **1993**, *17*, 266–278.
- (48) Shoichet, B. K.; Bodian, D. L.; Kuntz, I. D. Molecular Modeling Using Shape Descriptors. *J. Comput. Chem.* **1992**, *13*, 380–397.
- (49) Connolly, M.; Gschwend, D. A.; Good, A. C.; Oshiro, C.; Kuntz, I. D. DOCK 3.5, Department of Pharmaceutical Chemistry, University of California, San Francisco, CA, 1995.
- (50) The RELIbase service was used to retrieve the complexes filled with the following PDB entry codes: 1A82; 1B80; 1DAG; 1UOX; 1VFN; 1MUD; 1ZIN; 1DAH; 1BX4; 4HOH; 1KI5; 1AGR; 1QHI; 1GNQ; 1CLU; 1KI2; 1ULB; 1GNP; 1AZ1; 1RH3. RELIbase is a Web-based service to retrieve ligand/receptor structures deposited in the Brookhaven Protein Data Bank using substructure queries (<http://pdb.pdb.bnl.gov:8081/home.html>).
- (51) Bernstein, F. C.; Koetzle, T. F.; Williams, G. J. B.; Meyer, E. F., Jr.; Brice, M. D.; Rodgers, J. R.; Kennard, O.; Shimanouchi, T.; Tasumi, M. The Protein Data Bank: A Computer-Based Archival File for Macromolecular Structure. *J. Mol. Biol.* **1977**, *112*, 535–542.
- (52) Compound **III** was selected for docking because it features, similarly to the ATBI derivative **23**, an aromatic moiety filling the putative lipophilic L1 pocket and, similarly to compound **VII**, all the six hypothesized pharmacophoric elements.
- (53) Rivkees, S. A.; Barbhuiya, H.; IJzerman, A. P. Identification of the Adenine Binding Site of the Human A₁ Adenosine Receptor. *J. Biol. Chem.* **1999**, *274*, 3617–3621.
- (54) Townsend-Nicholson, A.; Schofield, P. R. A Threonine Residue in the 7th Transmembrane Domain of the Human A₁-Adenosine Receptor Mediates Specific Agonist Binding. *J. Biol. Chem.* **1994**, *269*, 2373–2376.
- (55) Tucker, A.; Robeva, A. S.; Taylor, H. E.; Holetton, D.; Bockner, M.; Lynch, K. R.; Linden, J. A₁ Adenosine Receptors-2 Amino acids are Responsible for Species-Differences in Ligand Recognition. *J. Biol. Chem.* **1994**, *269*, 27900–27906.
- (56) Olah, M. E.; Ren, H. Z.; Ostrowski, J.; Jacobson, K. A.; Stiles, G. L. Cloning, Expression, and Characterization of the Unique Bovine A₁ Adenosine Receptor-Studies on the Ligand Binding Site by Site-Directed Mutagenesis. *J. Biol. Chem.* **1992**, *267*, 10764–10770.
- (57) The orientation of **25** within the A₁AR binding site, as depicted in Figure 5, was obtained by a simple overlay of this ligand on the docked geometry of **23** about their common skeleton.
- (58) Mattos, C.; Ringe, D. Multiple Binding Modes. In *3D QSAR in Drug Design. Theory Methods and Applications*; Kubinyi, H., Ed.; ESCOM: Leiden, 1993; pp 117–136.
- (59) Kubinyi, H. Similarity and Dissimilarity: A Medicinal Chemist's View. In *3D QSAR in Drug Design. Ligand-Protein Interactions and Molecular Similarity*; Kubinyi, H., Folkers, G., Martin, Y. C., Eds.; KLUWER/ESCOM:1998; Vol. 2, pp 225–252.

- (60) Businelli, M. Metodi di Sintesi della *p*-Ossibenzaldeide a Partire da Fenolo. *Farmaco* **1950**, *5*, 522–527.
- (61) Hatanaka, M.; Ishimaru, T. Synthetic Penicillins. Heterocyclic Analogues of Ampicillin. Structure–Activity Relationships. *J. Med. Chem.* **1973**, *16*, 978–984.
- (62) Colotta, V.; Catarzi, D.; Varano, F.; Cecchi, L.; Filacchioni, G.; Martini, C.; Trincavelli, L.; Lucacchini, A. 1,2,4-Triazolo[4,3-*a*]quinoxalin-1-one: A Versatile Tool for the Synthesis of Potent and Selective Adenosine Receptor Antagonists. *J. Med. Chem.* **2000**, *43*, 1158–1164.
- (63) Pirovano, I. M.; IJzerman, A. P.; van Galen, P. J. M.; Soudijn, W. The Influence of Molecular Structure of N⁶-(*ω*-aminoalkyl)-adenosines on Adenosine Receptor Affinity and Intrinsic Activity. *Eur. J. Pharmacol.* **1989**, *172*, 185–193.
- (64) Cheng, Y. C.; Prusoff, W. H. Relation Between the Inhibition Constant K_i and the Concentration of Inhibitor which Causes Fifty Percent Inhibition (IC_{50}) of an Enzyme Reaction. *Biochem. Pharmacol.* **1973**, *22*, 3099–3108.
- (65) Sybyl Molecular Modelling System(version 6.2), Tripos Associates, St. Louis, MO.
- (66) Pearlman, D. A.; Case, D. A.; Caldwell, J. W.; Ross, W. S.; Cheatham T. E., III; Debolt, S.; Ferguson, D. M.; Seibel, G. L.; Kollman, P. A. AMBER, a Package of Computer Programs for Applying Molecular Mechanics, Normal-Mode Analysis, Molecular Dynamics and Free Energy Calculations to Simulate the Structural and Energetic Properties of Molecules. *Comput. Phys. Commun.* **1995**, *91*, 1–41.
- (67) Pearlman, D. A.; Case, D. A.; Caldwell, J. W.; Ross, W. S.; Cheatham T. E., III; Ferguson, D. M.; Seibel, G.; Singh, U. C.; Weiner, P. K.; Kollman, P. A. AMBER 4.1; Department of Pharmaceutical Chemistry, University of California: San Francisco, CA, 1995.
- (68) Kyte, J.; Doolittle, R. F. A Simple Method for Displaying the Hydrophobic Character of a Protein. *J. Mol. Biol.* **1982**, *157*, 105–132.
- (69) Baldwin, J. M. Structure and Function of Receptors Coupled to G Proteins. *Curr. Opin. Cell Biol.* **1994**, *6*, 180–190.
- (70) Schwartz, T. W. Locating Ligand-Binding Sites in 7TM Receptors by Protein Engineering. *Curr. Opin. Biotechnol.* **1994**, *5*, 434–444.
- (71) van Rhee, A. M.; Jacobson, K. A. Molecular Architecture of G Protein-Coupled Receptors. *Drug Dev. Res.* **1996**, *37*, 1–38.
- (72) Zhang, D.; Weinstein, H. Polarity Conserved Positions in Transmembrane Domains of G-Protein Coupled Receptors and Bacteriorhodopsin. *FEBS Lett.* **1994**, *337*, 207–212.
- (73) Berendsen, H. J. C.; Postma, J. P. M.; van Gunsteren, W. F.; DiNola, A.; Haak, J. R. Molecular Dynamics with Coupling to an External Bath. *J. Chem. Phys.* **1984**, *81*, 3684–3690.
- (74) Laskowski, R. A.; McArthur, M. W.; Moss, D. S.; Thornton, J. M. PROCHECK: A Program to Check the Stereochemical Quality of Protein Structures. *J. Appl. Crystallogr.* **1993**, *26*, 283–291.
- (75) Allen, F. H.; Bellard, S.; Brice, M. D.; Cartwright, B. A.; Doubleday, A.; Higgs, H.; Hummelink, T.; Hummelink-Peters, B. G.; Kennard, O.; Motherwell, W. D. S.; Rodgers, J. R.; Watson, D. G. The Cambridge Crystallographic Data Centre: Computer-Based Search, Retrieval, Analysis and Display of Information. *Acta Crystallogr.* **1979**, *B35*, 2331–2339.
- (76) Dewar, M. J. S.; Zebisch, E. G.; Healy, E. F.; Stewart, J. J. P. AM1: a New General Purpose Mechanical Molecular Model. *J. Am. Chem. Soc.* **1985**, *107*, 3902–3909.
- (77) MOPAC (version 6.0) is available from Quantum Chemistry Program Exchange, No. 455.
- (78) Connolly, M. L. Solvent-accessible Surfaces of Proteins and Nucleic Acids. *Science* **1983**, *221*, 709–713.
- (79) Connolly, M. L. Analytical Molecular Surface Calculation. *J. Appl. Crystallogr.* **1983**, *16*, 548–558.
- (80) Kuntz, I. D.; Blaney, J. M.; Oatley, S. J.; Langridge, R.; Ferrin, T. E. A Geometric Approach to Macromolecule-Ligand Interactions. *J. Mol. Biol.* **1982**, *161*, 269–288.
- (81) Cornell, W. D.; Cieplak, P.; Bayly, C. I.; Gould, I. R.; Merz, K. M.; Ferguson, D. M.; Spellmeyer, D. C.; Fox, T.; Caldwell, J. W.; Kollman, P. A. A Second Generation Force Field for the Simulation of Proteins, Nucleic Acids, and Organic Molecules. *J. Am. Chem. Soc.* **1995**, *117*, 5179–5197.
- (82) Joshi, K. C.; Jain, R.; Dandia, A.; Sharma, K. Synthesis of [1,2,4]-Triazino[4,3-*a*]benzimidazol-4(10H)-ones as Antimicrobial Agents. *Indian J. Chem.* **1989**, *28B*, 698–701.
- (83) IUPAC–IUB Commission on Biochemical Nomenclature. Abbreviations and Symbols for the Description of the Conformation of the Poly-Peptide Chains. *J. Mol. Biol.* **1970**, *52*, 1–17.

JM001054M